Mechanics and Mechanical Engineering
Vol. 14, No. 2 (2010) 325–337

Numerical Calculations of Stability of Spherical Shells

Tadeusz Niezgodziński
Department of Dynamics
Technical University of Łódź
Stefanowskiego 1/15, 90–924 Łódź, Poland

Jacek Świniarski
Department of Strength of Materials and Structures
Technical University of Łódź
Stefanowskiego 1/15, 90–924 Łódź, Poland

Received (13 June 2010)
Revised (15 July 2010)
Accepted (25 August 2010)

The results of FEM calculations of stability of thin–walled spherical shells are presented. A static and dynamic stability analysis was conducted. Hemispherical shells and spherical caps with various dilation angles, subjected to external pressure, were considered.

For each shell calculated, various boundary conditions of support were analyzed: joint, fixed and elastically fixed support. In the calculations, an axisymmetric and random discretization of the model was accounted for

As a result of the calculations conducted for static loads, values of upper critical pressures and buckling modes of the shells were obtained. The results were presented for various shell thicknesses.

The FEM solutions were compared to the available results obtained with analytical and numerical methods, showing a good conformity.

Dynamic calculations were conducted for a triangular pulse load. On the basis of the Budiansky–Roth dynamic criterion of stability loss, values of upper dynamic critical pressures were obtained. Shell buckling modes were determined as well.

Keywords: Structure stability, spherical shells, FEM

1. Introduction

Spherical shells are often applied in technological solutions. They are used as elements of pressure vessels (loaded with internal pressure) or roof coverings and domes (external pressure). In the present study, the problem of stability loss in spherical shells in aspect of their application to absorb blast wave energy (anti–blast protections) is considered. The stability problem of hemispheres and spherical segments is analyzed.

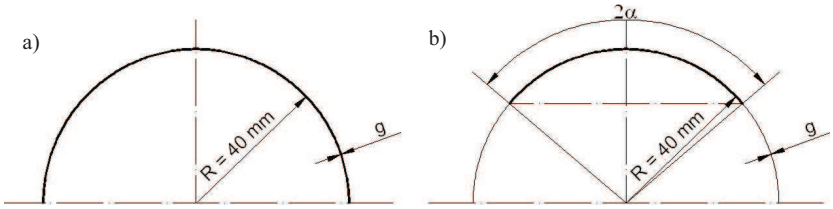

Figure 1 Geometrical dimensions of the spherical shells under consideration

Spherical shells made of steel of various sheet thickness from g = 0.1 mm to g = 1.0 mm were analyzed. The mechanical properties of steel were assumed as for St3 steel, namely:

- Young's modulus E = 200 GPa,
- Poisson's ratio $\nu = 0.3$,
- density $\rho = 7850$ kg/m^3.

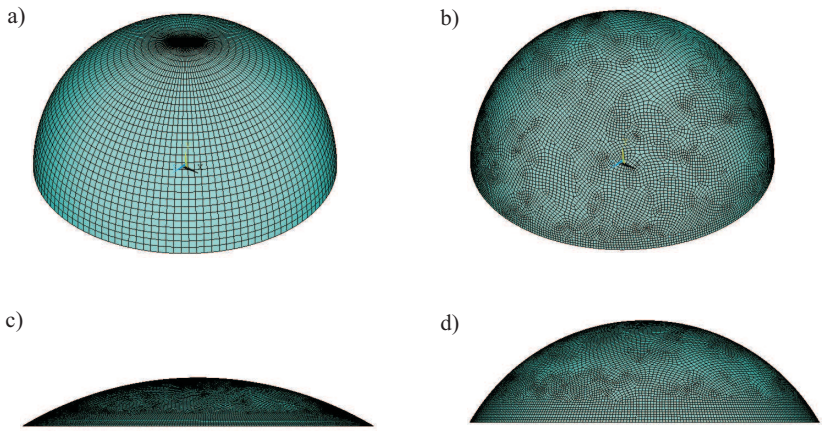

Figure 2 Division of a hemisphere and a spherical cap into finite elements
a)– axisymmetric division,
b) c) d) – random division.

2. Solution method

The stability problem was solved numerically with the finite element method. The FEM ANSYS 12.1 [6] package was employed. The FEM model was built with SHELL43 elements. Such an element enables modeling linear and nonlinear material properties. It also renders defining the material as a multilayer shell with a possibility to determine orthotropic properties of each layer possible.

Fig. 2 shows a division into finite elements. The computations were conducted both for an axisymmetric division and for a random division as the axisymmetric

division prefers the axially symmetrical deflection mode of the shell. In the case of the axisymmetric division, a regular mesh with quadrilateral, eight–node elements (SHELL43) with five degrees of freedom in each node was used [6]. A division into elements of the whole shell without entailing the axial symmetry with same elements was considered as well. The dimensions of the elements are comparable for both division cases. The finite elements were selected as to have at least 10 elements per each halfwave of the deformed shell.

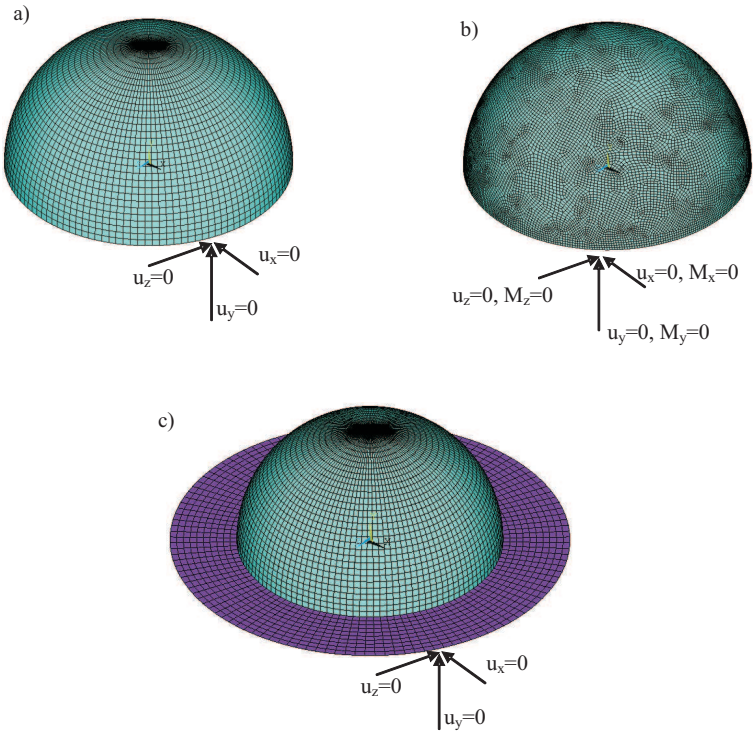

Figure 3 Boundary conditions assumed in the numerical computations
a) – joint support along the lower edge of the hemisphere,
b) – fixed support along the lower edge of the hemisphere,
c) – displacements $u_x = u_y = u_z = 0$ along the "hat rim" circumference.

The computations were conducted for various boundary conditions of the shell support. The following kinds of boundary conditions shown in Fig. 3 were considered:

1. joint support (Fig. 3a),

2. fixed support (Fig. 3b),

3. elastically fixed support – the so-called "hat with a rim" (Fig. 3c).

3. Calculations of the static stability

Calculations of the stability for static loads were conducted to validate the numerical models and to determine the uppermost values of critical loads and buckling modes. The calculations were carried out for the load in the form of uniform external pressure.

In Fig. 4 values of critical pressure as a function of wall thickness of the hemisphere jointly supported along the base circumference are listed. This solution corresponds to the model with an axisymmetric division into fine elements and perfectly agrees with the well known Zoelly- Leibenson formula [3],[7] :

$$p_{cr}^{o} = \frac{2E}{\sqrt{3(1-\nu^2)}} \left(\frac{g}{R}\right)^2$$

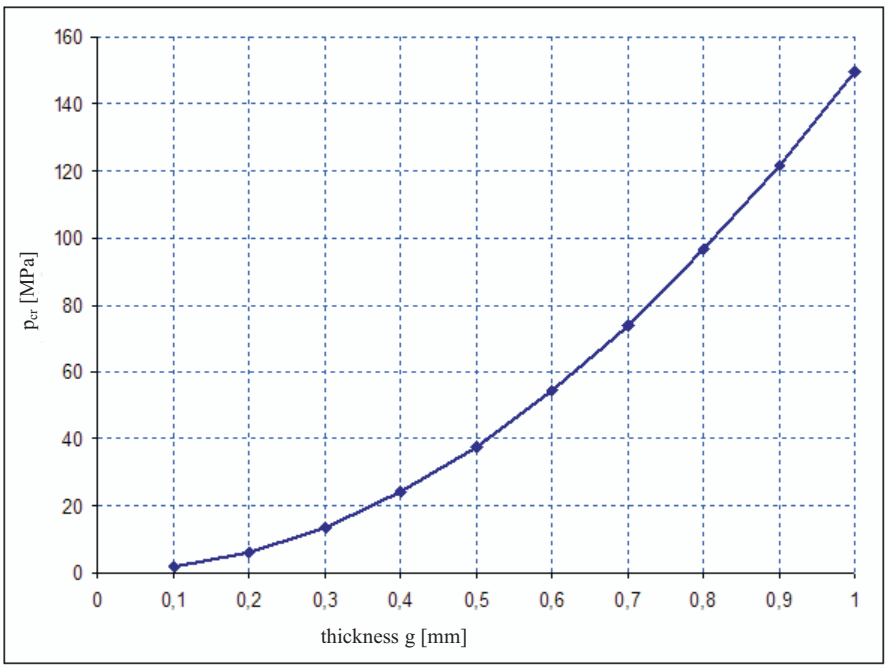

Figure 4 Values of upper critical pressures versus the hemisphere wall thickness.

For the hemisphere of the wall thickness exceeding 0.2 mm, the effective stresses (corresponding to the critical pressure of 6 MPa) are slightly higher than 700 MPa, which disqualifies this solution if buckling in the elastic range is of interest.

Further on, the calculations of critical buckling modes of the hemisphere of the wall thickness in the range from 0.1 mm to 1.0 mm were conducted. The results are presented in Figs. 5 and 6.

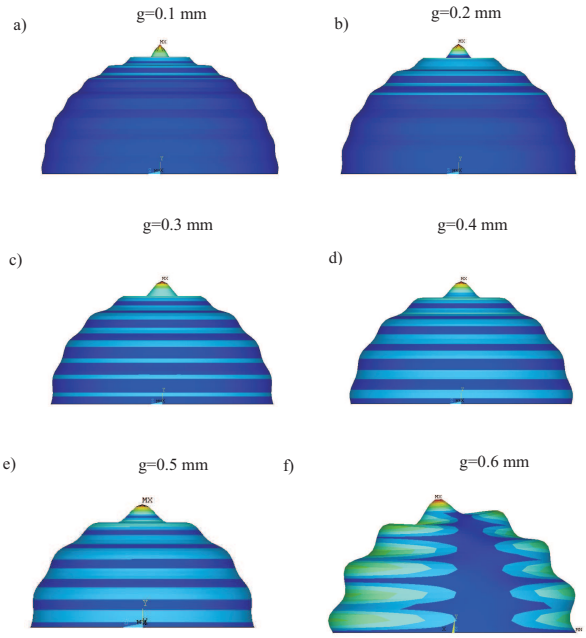

Figure 5 Critical modes for the hemisphere wall thickness from 0.1 to 0.6 mm

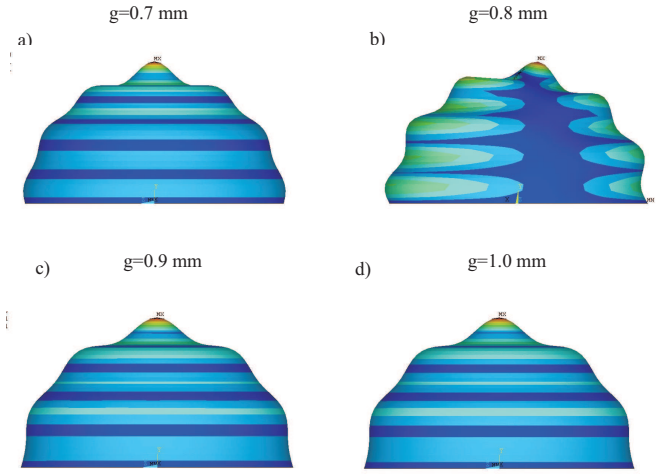

Figure 6 Critical modes for the hemisphere wall thickness from 0.7 to 1.0 mm

Attention should be paid to the fact that the mode corresponding to the lowest value of the upper critical load depends on the way the model is divided into finite elements. The axisymmetric division entails the axisymmetric mode. An exception is the solution presented in Figs. 6.a and 6.d, where the antisymmetry plane can be seen.

Higher values of critical pressures and their corresponding buckling modes were calculated as well. Those calculations were conducted for the hemisphere with the wall thickness of g = 0.1 mm. First six critical modes are shown in Fig. 7.

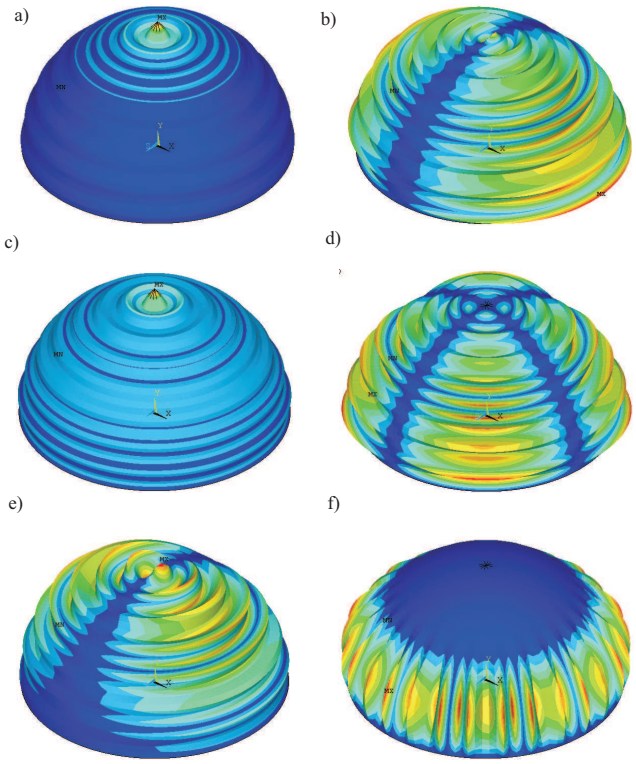

Figure 7 Critical modes (from 1 to 6) for the hemisphere of the wall thickness equal to 0.1 mm

Values of critical pressure that correspond to the subsequent eleven modes of buckling were also calculated. These values are listed in Tab. 1. Attention should be drawn to the fact that subsequent values of critical load are situated very close to one another. A difference in values of critical loads for the first eleven eigenmodes does not exceed 3%. On the basis of the analytical solutions given in [7], the calculations of stability of a segment of the spherical shell shown in Fig. 1.b. were conducted. In the above–mentioned monograph it is said that the upper critical load of the hemisphere and spherical segment for the angle $\alpha > 20^o$ are equal to each other.

Table 1 Values of upper critical loads of the hemisphere under external pressure

No.	p_{cr} [MPa]	difference % [-]
1	1.516788	0
2	1.528984	0.79
3	1.534597	1.16
4	1.540514	1.54
5	1.549312	2.09
6	1.554015	2.39
7	1.55447	2.42
8	1.555077	2.46
9	1.560386	2.79
10	1.560538	2.80
11	1.560993	2.83

Table 2 Values of critical loads

Analytical-numerical solution for spherical cap 2α=60 $^\circ$ p_{cr} [MPa]						
g [mm]	solution from [2]	Joint support, non-linear precritical state [2]		Fixed support, non-linear precritical state [2]		
0.1	1.513	1.12 / 1.06		1.22 / 1.17		
0.2	6.05	4.79 / 4.25		4.87 / 4.67		
0.3	13.62	10.79 / 9.57		10.96 / 10.51		
0.4	24.21	19.17 / 17.02		19.49 / 18.69		
FEM solution p_{cr} [MPa]						
g [mm]	Hemisphere joint support, axial symmetry of elements	Hemisphere joint support, random division	Hemisphere fixed support, axial symmetry of elements	Hat	Spherical cap 2α=60^o	Spherical cap 2α=120^o
0.1	1.51 (Fig.8a)	1.528 (Fig.8e)	1.51 (Fig.8i)	1.51	1.53 (Fig.8m)	1.527
0.2	6.04 (Fig.8b)	6.086 (Fig.8f)	6.05 (Fig.8j)	6.06	6.08 (Fig.8n)	6.095
0.3	13.57 (Fig.8c)	13.64 (Fig.8g)	13.6 (Fig.8k)	13.60	13.75 (Fig.8p)	13.706
0.4	24.08 (Fig.8d)	24.21 (Fig.8h)	24.16 (Fig.8l)	24.16	24.40 (Fig.8r)	24.293

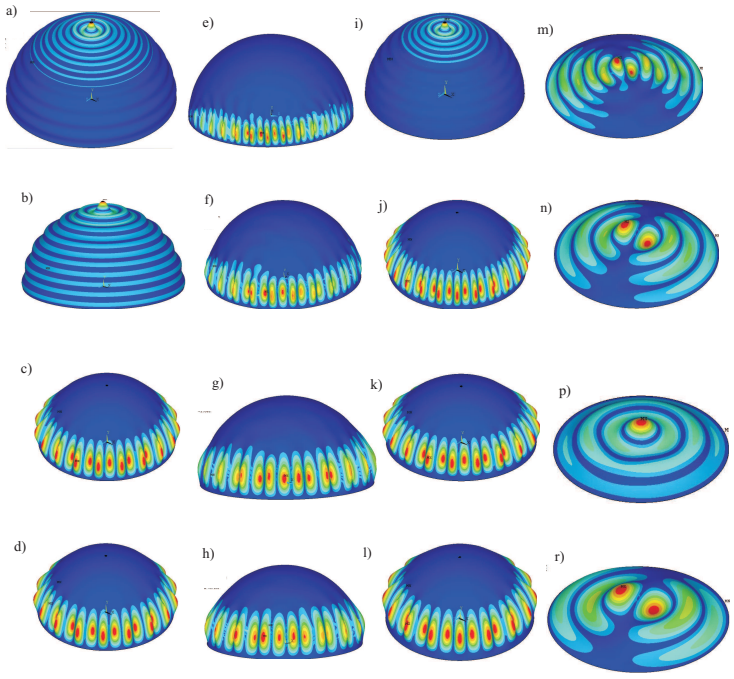

Figure 8 Selected buckling modes of the hemisphere for various boundary conditions (Tab. 2)

Values of critical loads determined with analytical methods and the FEM are presented in Tab. 2. Those values were calculated for various boundary conditions mentioned in the Tab. 2 headings. Buckling modes corresponding to the values of critical pressures are presented in Fig. 8 and described in Tab. 2.

A good conformity between the values of critical loads obtained for the linear critical state with the analytical method and the FEM has been found.

Also, the numerical calculations for the load with pressure varying according to the cosine function from the maximum value at the highest point on the shell to zero at the base were conducted. It corresponds only to the normal component of the pressure wave acting along the shell axis.

In Table 3 and in Fig. 9, values of critical loads versus the wall thickness for the uniform pressure load and for the pressure load that varies according to the cosine function are presented. As can be seen, the differences in critical pressure values are inconsiderable. The differences are exemplified only by the shape of buckling modes. This phenomenon has been described by Volmir [7]. On the basis of observations and experiments conducted, it has been found that the spherical shell upper part defined by the angle $2\alpha = 60^o$ according to Fig. 1.b decides mainly about its stability loss. In the case under analysis, all kind of loads cover the surface with the maximum load value, hence, we have such a behavior of the system. Although

the way the load is applied does not affect the critical mode, it will influence the postcritical behavior of the hemisphere or the spherical cap.

An effect of alternations in the base diameter at the constant model height was also considered. This assumption followed from the requirements imposed by applications in anti–blast protections. The constant height of the spherical segment was assumed as $H = 40$ mm, whereas the base diameter varied within the range from $2R = D = 80$ mm to $D = 120$ mm, every 10 mm. The structure was subject to the pressure distributed according to the cosine function.

Table 3 Values of the hemisphere critical pressure

g [mm] wall thickness	P_{cr} [MPa] uniform distribution	P_{cr} [MPa] distribution according to the cosine function
0.1	1.513	1.520
0.2	6.058	6.099
0.3	13.637	13.749
0.4	24.225	24.480

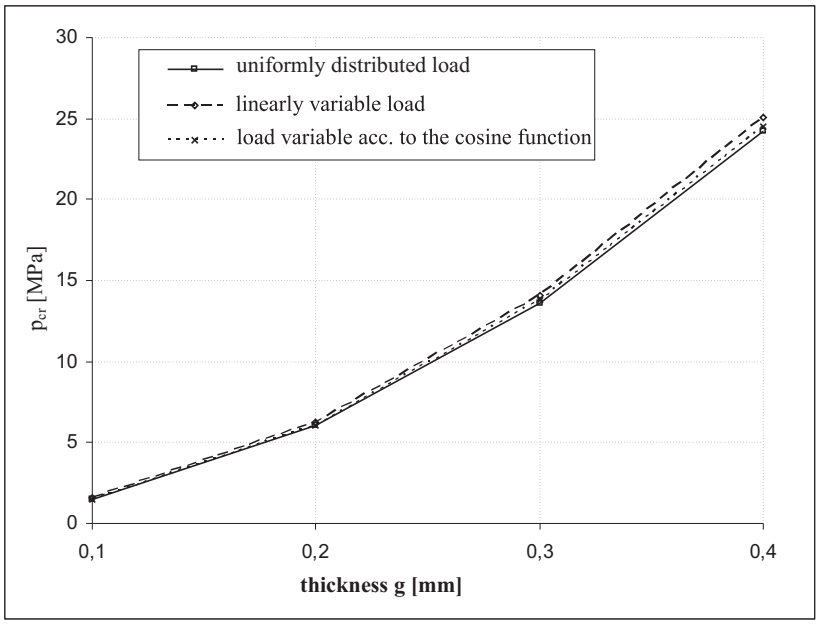

Figure 9 Critical pressure values for the hemisphere

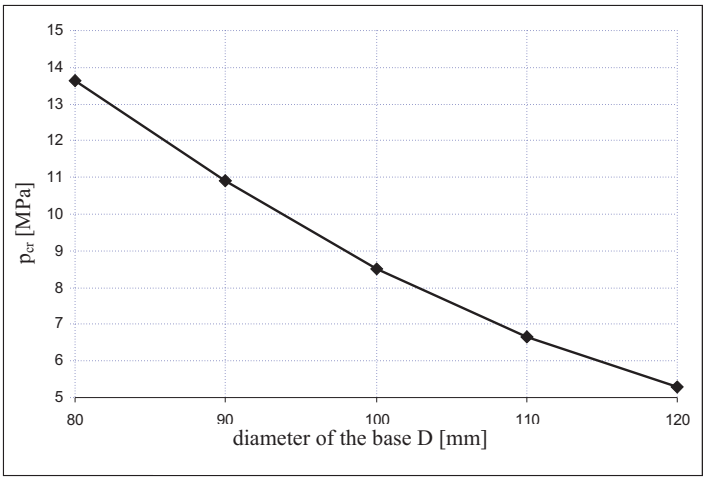

Figure 10 Upper critical pressure as a function of the base diameter (the spherical segment of constant height H=40 mm)

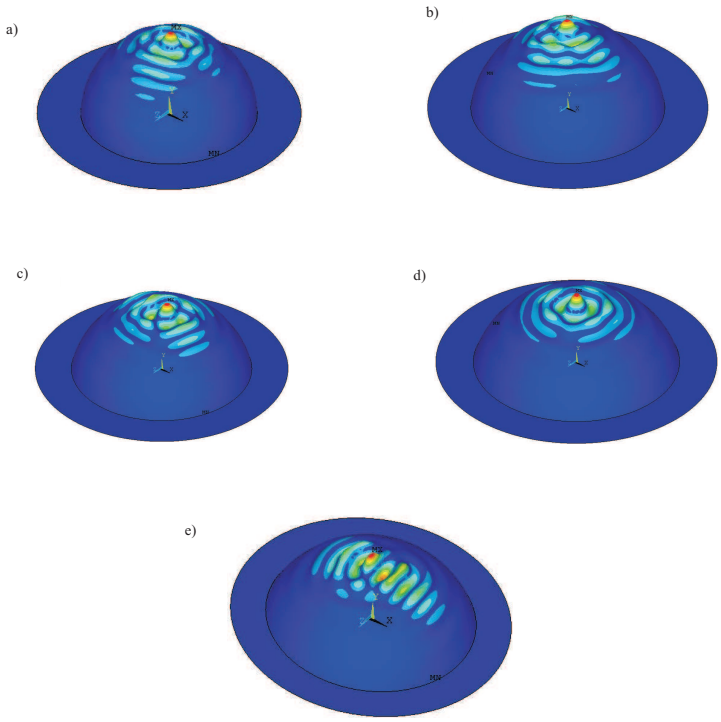

Figure 11 Critical modes for the spherical segment under uniform pressure base diameter from 80 mm (Fig. a) to 120 mm (Fig. e)

The results for the wall thickness $g = 0.3$ mm are presented in Fig. 10 and the buckling modes are shown in Fig. 11.

The value of the critical load decreases with an increase in the base diameter. The model changes from a hemisphere to a spherical cap of the base diameter of $D = 120$ mm. An increase in the base diameter by 50 % was followed by a decrease in the critical load from approx. 13.5 MPa for the hemisphere to approx. 5 MPa for the spherical segment with the base diameter $D = 120$ mm. Simultaneously, a change in the buckling mode from the symmetrical one presented in Fig. 11.a into the non–symmetrical one shown in Fig. 11.e can be seen.

4. Calculations of the dynamic stability

The dynamic calculations were conducted for a triangular pulse load with the load increase time of 0.05 ms and the total pulse duration of 0.5 ms.

On the basis of the Budiansky–Roth dynamic stability loss criterion (see [1], [4], [5]), values of dynamic critical loads were obtained. In the calculations, the dynamic load factor (DLF) defined as a ratio of the dynamic load amplitude to the static bifurcation load, was used. Modes of shell buckling were determined as well.

For the jointly supported shell (Fig. 3.a) of the wall thickness g = 0.3 mm, dynamic buckling characteristics was prepared. The system load is a uniform pressure distribution on the whole surface of the shell. The pulse duration is comparable to the free vibration period.

A plot depicting values of the dimensionless maximum deflection of the hemisphere as a function of the dynamic load factor (DLF) is shown in Fig. 12.

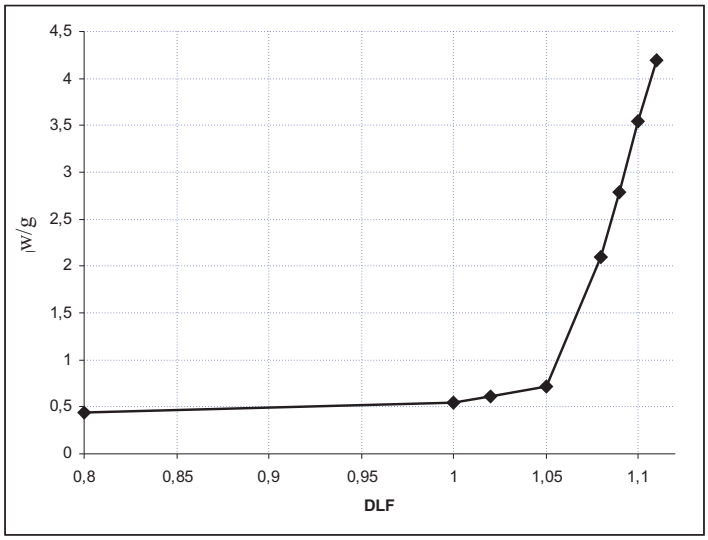

Figure 12 Plot of the dimensionless maximum deflection of the hemisphere versus the DLF. Initial deflection w/g = 0.01; pulse duration t = 0.09 ms. Static upper critical load p_{cr}=13.6 MPa.

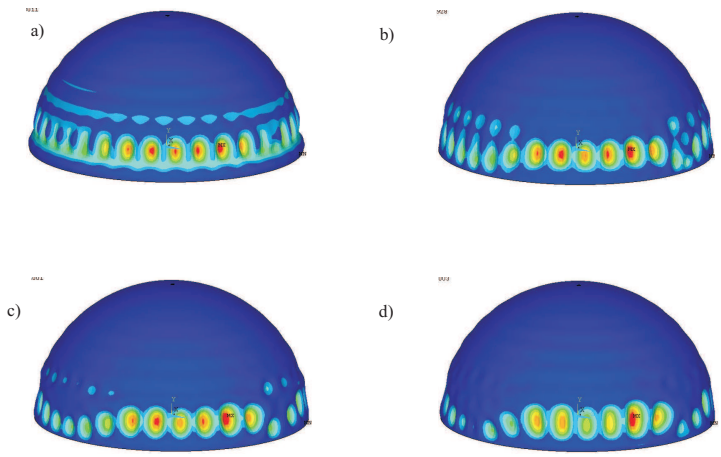

Figure 13 Deflections for the DLF = 1.08 after:
a) 0.022 ms b) 0.024 ms c) 0.026 ms c) 0.028 ms, respectively

The shape of the shell deflection for the value of the DLF = 1.08 at four time instants is presented in Fig. 13.

5. Conclusions

The results of the numerical calculations of static and dynamic stability of hemispherical shells subjected to external pressure are presented. It was found that numerous first values of critical loads corresponding to different buckling modes stay very close each other (up to 3%). It shows a very considerable impact of initial imperfections on deflection modes, but not on the value of critical pressure.

In dynamic analysis a triangular pulse load was assumed. The Budiansky – Roth dynamic stability criterion was used. As a result of the calculations, values of the dynamic critical pressure and buckling modes were obtained each time.

The calculation results are the basis for further investigations of blast energy absorption by lightweight protections. Such protections will be composed of a system of hemispherical shells. The main problem is a stability loss in shells and considerable plastic deflections that cause a decrease in the total reaction of the background.

References

[1] **Budiansky, B. and Roth, R.S.**: Axisymmetric dynamic buckling of clamped shallow spherical shell, Collected papers on instability of structures, NASA TN D-1510, 591–600, **1962**.

[2] **Grigoljuk, E. and Kabanow, W.**: Stability of shells, (in Russian), *Science*, Moscow, **1978**.

[3] **Marcinowski, J.**: Stability of relatively deep segments of spherical shells loaded by external pressure, *Journal of Thin Walled Structures*, 45, 906–910, **2007**.

[4] **Simitses, G.J.**: Buckling of moderately thick laminated cylindrical shell: a Review, Composites Part B, 27 B, 581–587, **1996**.

[5] **Simitses, G.J.**: Dynamic stability of suddenly loaded structures, *Springer Verlag*, New York, **1990**.

[6] User's Guide ANSYS 12.1. Ansys. Inc.. Houston. USA

[7] **Volmir, A.S.**: Stability of deformed bodies, (in Russian), *Science*, Moscow, **1967**.